analytical chemistry

Article

pubs.acs.org/ac

2D Photonic Crystal Protein Hydrogel Coulometer for Sensing Serum Albumin Ligand Binding

Zhongyu Cai, Jian-Tao Zhang, Fei Xue, Zhenmin Hong, David Punihaole, and Sanford A. Asher*

Department of Chemistry, University of Pittsburgh, Pittsburgh, Pennsylvania 15260, United States

Supporting Information

ABSTRACT: Bovine and human serum albumin (BSA and HSA) are globular proteins that function as bloodstream carriers of hydrophobes such as fatty acids and drugs. We fabricated novel photonic crystal protein hydrogels by attaching 2D colloidal arrays onto pure BSA and HSA hydrogels. The wavelengths of the diffracted light sensitively report on the protein hydrogel surface area. The binding of charged species to the protein hydrogel gives rise to Donnan potentials that change the hydrogel volume causing shifts in the diffraction. These photonic crystal protein hydrogels act as sensitive Coulometers that monitor the hydrogel charge state. We find multiple high-affinity BSA and HSA binding sites for salicylate, ibuprofen and picosulfate by using these sensors to monitor binding of charged drugs. We demonstrate proof-of-concept for utilizing protein hydrogel sensors to monitor protein−ionic species binding.

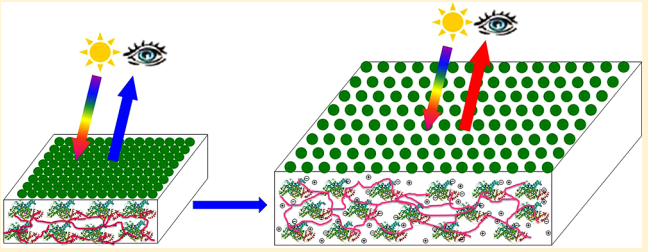

There is intense interest in developing sensing technologies capable of visually identifying and quantifying chemical or biological agents.[1−5] The ideal sensing technology would be highly selective and appropriately sensitive to the analyte concentrations of interest. The existing chemical and biological sensing technologies often combine recognition chemistry, amplification chemistry and spectroscopic or electrochemical readouts.[5−10]

We previously pioneered 3D crystalline colloidal array (CCA) photonic crystal sensing materials that utilized responsive hydrogel materials.[11−13] We fabricated responsive hydrogels by attaching molecular recognition agents to hydrogels containing 3D photonic crystals. The fragility of the 3D CCA formation process was quite limiting for this 3D CCA photonic crystal sensing technology. We recently discovered a new sensing motif that utilizes highly efficient diffraction from a 2D array monolayer of submicrometer dielectric particles placed on top of chemically responsive hydrogels.[14,15] This diffraction sensitively monitors the 2D array particle spacing as the hydrogel volume varies in response to changes in its chemical environment.[15−17] In stark contrast to the 3D array self-assembly process that requires nonionic, chemically and physically gentle fabrication conditions, the 2D array photonic crystal hydrogel fabrication decouples the 2D CCA fabrication from the responsive hydrogel synthesis.[16] This decoupling of the responsive hydrogel synthesis from the 2D array fabrication allows us, for the first time, to directly use proteins to fabricate responsive hydrogels by directly cross-linking proteins and placing 2D arrays on their surfaces.

Among various responsive hydrogels, protein-linked hydrogels have received a great deal of attention because of their molecular recognition abilities and intelligent response to external stimuli. "Smart" hydrogels containing proteins have been fabricated to take advantage of the protein selective chemistry or ligand binding for bioanalytical sensing. There are a few reports of using the protein conformational response for sensing applications.[18−22] Most of these studies attached proteins to hydrogels or cross-linked proteins within hydrogels. Bovine serum albumin (BSA) and human serum albumin (HSA) are globular proteins that are used in numerous biochemical applications due to their stability, low cost and ligand binding properties.[23] In the present work, we describe the fabrication of novel 2D photonic crystal BSA and HSA protein hydrogels for sensing applications. The sensor readout utilizes light diffraction from 2D CCA. We believe that our work is the first to demonstrate functional hydrogel formation directly from proteins for sensing applications. We also recognize that numerous protein hydrogels have been developed in recent years for areas such as tissue engineering.[24−26] Our protein hydrogels act as Coulometers to detect the binding of charged species. Our protein hydrogels also change volume in response to chelating agents that form protein cross-links.

EXPERIMENTAL SECTION

Materials. Styrene, bovine and human serum albumin (BSA and HSA, essentially fatty acid free), sodium dodecyl sulfate (SDS), dodecyltrimethylammonium bromide (DTAB), dodecyl octaethylene glycol ether ($C_{12}E_8$), dodecanol, 1-propanol, sodium chloride, calcium chloride dehydrate, sodium salicylate, ibuprofen, and sodium dodecanoate (SD) were purchased from

Received: December 19, 2013
Accepted: April 25, 2014
Published: April 25, 2014

Sigma-Aldrich and were used as received. Sodium picosulfate was purchased from BOC Sciences. Glutaraldehyde (50 wt % in water) was purchased from Sigma-Aldrich and diluted into a 25 wt % aqueous stock solution prior to use. Ultrapure water with resistivity >18.2 MΩ·cm^{-1} was obtained from an ultrapure water system (Barnstead). Glass slides (25 mm × 75 mm × 1 mm) were purchased from Fisher Scientific.

Preparation of 2D CCA-BSA and HSA Hydrogels. Figure 1 illustrates the fabrication of 2D CCA-BSA and -HSA protein hydrogel films for sensing applications, including the preparation of the 2D CCA, and cross-linking the BSA and HSA hydrogels with glutaraldehyde. This BSA and HSA protein hydrogel films can be cross-linked from solutions layered onto 2D close-packed CCA.

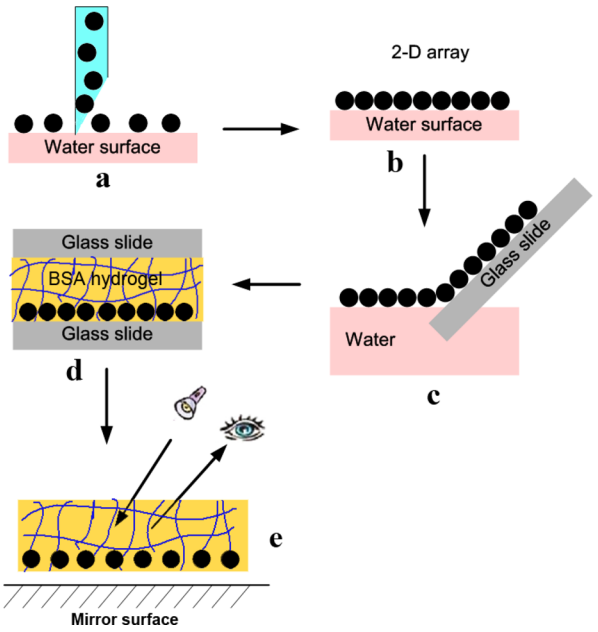

Figure 1. Fabrication of 2D CCA-BSA or -HSA protein hydrogel Coulometer sensors. (a) PS colloidal particle dispersion is layered onto a water surface. (b) The dispersion spreads to form a 2D close-packed CCA monolayer on the water surface. (c) 2D CCA is transferred to a glass slide. (d) BSA or HSA solution is layered on the 2D CCA and cross-linked to form a protein hydrogel. (e) The 2D CCA-BSA or -HSA hydrogel sensor is peeled off the glass slide and placed on a mirror that induces bright 2D array light diffraction.

Polystyrene (PS) colloidal spheres of ∼580 nm diameter were synthesized by using an emulsifier free emulsion polymerization method.[27] The 2D CCAs were fabricated by using our needle tip flow technique.[16] Typically, the PS colloidal dispersion (15 wt %) and 1-propanol were mixed at a volume ratio of 2:1 and the mixture vortexed for 1 min. Twenty microliters of this suspension was slowly and evenly layered on top of an ultrapure water surface in a 125 mm (in diameter) glass dish where it assembled into a hexagonal close-packed 2D CCA monolayer. This 2D CCA monolayer was transferred onto a wet glass slide.

BSA or HSA hydrogels were polymerized onto the 2D CCA on glass slides. Typically, 0.2 g BSA or HSA was dissolved in 1 mL phosphate buffer (PB, pH = 7.4, 0.1 M), giving a very light yellow solution. Typically, 8−20 μL of glutaraldehyde (25 wt %) cross-linker, was added to 0.5 mL BSA or HSA solution (2−5 wt % BSA/HSA). The solution was vortexed for 2 s and then layered onto the 2D CCA on the glass slide. Another glass slide was quickly placed onto the 2D CCA-BSA or -HSA solution. The reaction was carried out for 3 h at room temperature. The resulting yellow 2D CCA-BSA or -HSA hydrogel films were peeled off the glass slides, and washed with large amounts of PB (pH = 7.4, 10 mM) for at least 24 h, during which the buffer solution was frequently replaced (≥3 times).

Characterization. The ordering and morphology of the 2D CCA arrays were measured using an SEM (Joel JSM6390LV) after gold layer sputtering. The 2D CCA-BSA/HSA protein hydrogel was dried in the air, and then coated with a 30 nm thick gold layer for SEM measurements. Debye ring diffraction was utilized to determine the particle spacing. A 532 nm green laser pointer illuminated the surface of the 2D CCA-BSA/HSA protein hydrogel at normal incidence. The pH values were measured at room temperature (25 °C) using an Orion 3 Star pH meter (Thermo Electron Corporation).

The response of the 2D CCA-BSA protein hydrogel was detected by either measuring the diffraction wavelength with a reflection probe[17] or by measuring the Debye diffraction ring diameter as shown in Supporting Information Figure S1. For a close packed hexagonal 2D lattice, the distance between adjacent particles is equal to the PS sphere diameter, d. The maximum 2D interplanar distance is equal to d sin 60°. A single-domain 2D lattice will show six diffraction spots on a screen parallel to the 2D array. In contrast, small randomly oriented multidomain 2D lattice monolayers show Debye diffraction ring patterns.[28,29] The 2D CCA PS particle spacing can be calculated from the measured diameter of the ring, D, on a screen spaced a distance h from the 2D array. The ring diameter, D, depends upon the particle spacing, d, through the modified Bragg diffraction equation:

$$\sin \alpha = \frac{2\lambda}{\sqrt{3}\,d}$$

where α is the angle subtended by the Debye diffraction from the 2D CCA normal, λ is the laser wavelength, and d is the particle spacing. The diffraction angle α, can be determined from $\alpha = \arctan D/2h$, where h is the distance of the screen to the 2D CCA.[28] Thus, one can easily determine the 2D CCA particle spacing from

$$d = \frac{4\lambda\sqrt{(D/2)^2 + h^2}}{\sqrt{3}\,D}$$

The 2D CCA-BSA and -HSA protein hydrogels were cut into 8 mm × 8 mm pieces for the sensing measurements (glutaraldehyde content in these hydrogels is 3.5 wt % of BSA/HSA). For pH response measurements, the 2D CCA-BSA hydrogels were equilibrated in 30 mL PB (10 mM) at the pH 2 to 10.5 pH values at room temperature. For the SDS, DTAB, $C_{12}E_8$, and SD response studies, the BSA protein hydrogels were equilibrated in 30 mL SDS, DTAB, $C_{12}E_8$ or SD solutions at concentrations between 0 to 15 mM in PB (50 mM at pH = 8.0). For Ca^{2+} studies, the BSA protein hydrogels were equilibrated in 30 mL ultrapure water at $CaCl_2$ concentrations between 0 to 5 mM. For the drug measurements, the BSA/HSA protein hydrogels were equilibrated in 20 mL PB (50 mM at pH = 8.0) at drug concentrations between 0 and 9 mM. After equilibration the BSA protein hydrogels were placed on a glass slide and illuminated with a laser pointer (λ = 532 nm) to determine the Debye ring diameters. The Debye ring diameters

dx.doi.org/10.1021/ac404134t | Anal. Chem. 2014, 86, 4840−4847

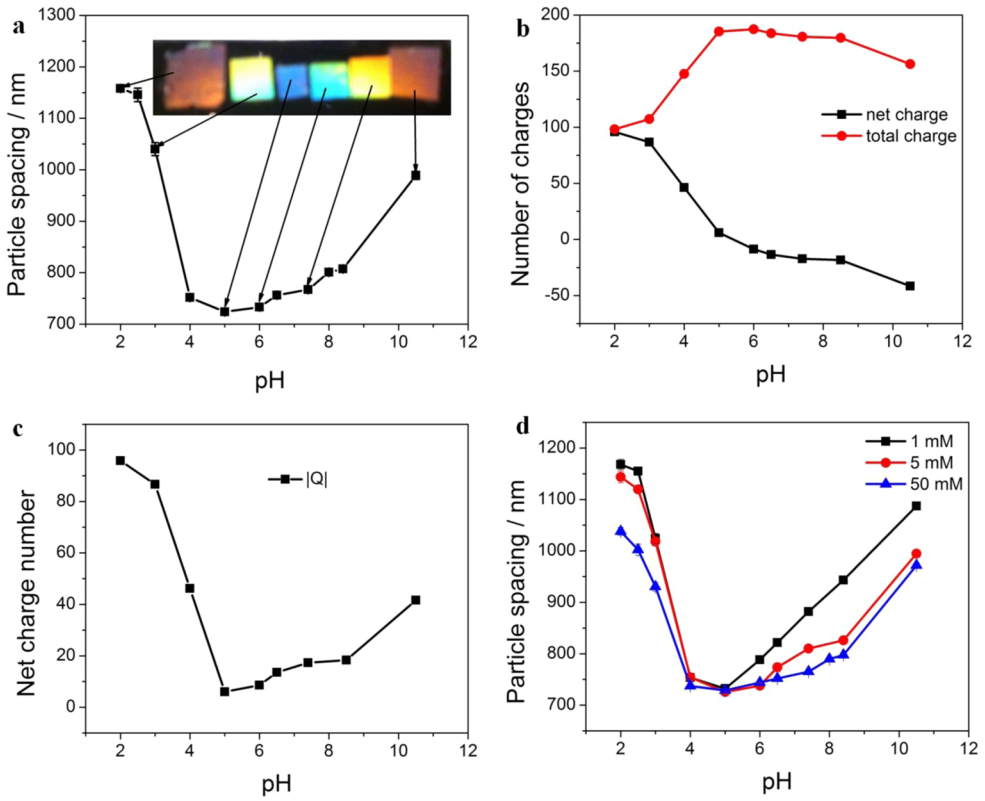

Figure 2. 2D CCA-BSA protein hydrogel pH dependence. (a) pH dependence of the particle spacing of the 2D CCA-BSA protein hydrogel in PB (10 mM). The inset shows photographs of the forward diffraction taken with a camera along the normal and the source below at an angle of 70° to the 2D array normal. (b) Calculated pH dependence of the total number of charges and the net charge. (c) Calculated BSA absolute value of net charge |Q|. (d) pH dependence of the 2D CCA-BSA hydrogel particle spacing at 1, 5, and 50 mM PB concentrations.

were measured at 9 different positions of each sample. The average and standard deviations are plotted in the figures.

UV Resonance Raman (UVRR) and Fluorescence Spectroscopy. The BSA monomer solution and hydrogel were characterized with UVRR and fluorescence to compare the protein conformation between the protein hydrogel and the native protein in solution. The UVRR measurements utilized a tunable Ti: sapphire laser (Photonics Industries) operating at 1 kHz to generate ~204 nm excitation by mixing the third harmonic with the ~816 nm fundamental. The laser light was focused onto a spinning Suprasil quartz NMR tube containing the sample. A ~165° backscattering geometry was used; the scattered light was imaged into a home-built subtractive double monochromator[30] and detected with a liquid N_2 cooled, back-thinned Spec-10:400B CCD camera (Princeton Instruments) with a Lumogen E coating.

The tryptophan (Trp) fluorescence spectra were acquired using a HORIBA Jobin Yvon Fluorolog-3 spectrofluorometer equipped with a Hamamatsu R928 detector. The emission spectra in the range of 305−450 nm were collected using 295 nm excitation with a 2.5 nm band-pass (for both excitation and emission).The sample was contained in a 1.0 cm × 1.0 cm quartz cuvette. The spectra were recorded at 0.5 nm data intervals and smoothed over 30 data points (15 nm) by using the Savitzky−Golay method.

RESULTS AND DISCUSSION

Our protein hydrogel sensors were prepared by glutaraldehyde cross-linking of BSA and HSA solutions layered onto a 2D close-packed CCA of 580 nm PS particles (Supporting Information Figure S2a) as shown in Figure 1. The resultant protein sensors show iridescence under white light illumination (Supporting Information Figure S3) because of the 2D CCA arrays on their surfaces (Supporting Information Figure S2b). The 2D CCA remains ordered as the spacing between particles changes. Debye ring diameters were used to measure the change in the surface area of the 2D photonic crystal protein hydrogel (Experimental Section and Supporting Information Figure S1). The response of the hydrogel is inversely correlated with the cross-linker concentration used (Supporting Information Figure S4).

2D CCA-BSA Protein Hydrogel pH Dependence. Figure 2a shows the pH dependence of the 2D CCA-BSA hydrogel particle spacing in 10 mM PB solution as determined by the Debye ring diameter (Supporting Information Figure S1). At pH 2, the BSA protein hydrogel is maximally swollen with a 2D CCA particle spacing of ~1120 nm. The spacing decreases to ~740 nm at pH 5, and slightly increases until ~pH 7, whereupon the particle spacing rapidly increases as the pH further increases. At pH 10.5, the 2D CCA particle spacing increases to ~970 nm (Figure 2a). The minimum particle spacing of ~740 nm, occurs close to the BSA isoelectric point (pI), while above and below the pI value, the protein hydrogel swells because of its increased side chain ionization.

The inset in Figure 2a shows that the forward diffracted color of the 2D CCA-BSA hydrogel shifts from violet toward red as the pH increasingly differs from its pI value. The color observed can be used to visually determine the particle spacing. The pH dependence is fully reversible between pH 2.0 to 10.5; we pH cycled the BSA protein hydrogel sensor 3 times over a period of

dx.doi.org/10.1021/ac404134t | Anal. Chem. 2014, 86, 4840−4847

156 h and observed essentially identical responses (Supporting Information Figure S5).

Our protein hydrogels have a lifetime of over 12 months when stored in a 4 °C refrigerator in cases where we used a modest attempt to avoid bacterial contamination.

BSA (HSA) is a 66 411 D (66 438 D) globular protein of 583 (585) amino acids,[31] many of which titrate between pH 2 and pH 12; there are 99 carboxylic acid groups (59 (60) Glu with $pK_a \approx 4.15$ and 40 (39) Asp with $pK_a \approx 3.71$). There are 99 (97) basic residues (59 (58) Lys with $pK_a \approx 10.67$, 23 (23) Arg with $pK_a \approx 12.5$ and 17 (16) His with $pK_a \approx 6.04$). We calculated the pH dependence of the BSA molecule total charge and net charge as shown in Figure 2b and c. Figure 2b shows the pH dependence of the actual net charge as well as the total number of charges, while Figure 2c shows the calculated pH dependence of the BSA protein absolute value of net charge, |Q| (absolute value of summed positive and negative charges).

The pH dependence of the BSA hydrogel 2D array spacing (Figure 2a) roughly tracks the pH dependence of the absolute value of the total net charge (Figure 2c). Increasing the pH from 2 to 5 decreases the number of positive charges and increases the number of negative charges. The hydrogel volume seems to little depend on the sign of the net charge or the number of total charges (Figure 2b).

The photonic crystal BSA protein hydrogel, thus, acts as a Coulometer where the particle spacing indicates the protein's charged state. From the slope of the dependence of the particle spacing on the protein charge, we calculate for the pH 2 to pH 4 region a BSA charge sensitivity of ~8.2 nm/charge in 10 mM PB. Between pH 6 and pH 10.5, we roughly calculate a somewhat smaller sensitivity of ~7.8 nm/charge in 10 mM PB (see Supporting Information for details of the calculation of charge sensitivities). The decreased sensitivity at higher pH presumably results from the increased high PB ionic strength (Supporting Information Table S1).

The 2D CCA-BSA protein hydrogel acts as a solution Coulometer by sensitively detecting changes in the net protein charge. The mechanism of the volume dependence on charge partially derives from the Donnan potential associated with excess hydrogel counterion concentrations over that existing in the solution reservoir.[32] The fact that the particle spacing scales better with the absolute value of the net charge than the total charge suggests that side chain ion pairing is important in determining the pH dependence of the BSA hydrogel volume.

We investigated the impact of the solution ionic strength on the charge dependence of the 2D CCA-BSA protein hydrogel particle spacing, using 1, 5, and 50 mM PB concentrations. As shown in Figure 2d, the pH dependence of the particle spacing appears very similar between pH 2 and 4, but the pH dependence decreases for the higher PB buffer concentrations between pH 6 through pH 10.5. The particle spacings at the higher PB concentrations are in general somewhat smaller than those at lower PB concentrations at the same pH. At pH 2, the 2D CCA-BSA protein hydrogel particle spacing in 50 mM PB (~1050 nm) is somewhat smaller than at lower PB concentrations (~1150 nm) because of the increased PB ionic strengths, that decrease the Donnan potential of the BSA protein hydrogel, leading to a decreased swelling.[32] However, these results indicate only a modest decrease in response sensitivity to charge, indicating that <50 mM PB ionic strengths have only modest impacts on the BSA hydrogel volume changes that result from protein net charge changes. The ionic strength values at different PB concentrations are shown in Supporting Information Table S1.

2D CCA-BSA Hydrogel SDS and DTAB Binding. Figure 3a shows the dependence of the 2D CCA-BSA hydrogel particle spacing on the binding of the anionic surfactant SDS. SDS, which binds to BSA with a high affinity ($K = 1.2 \times 10^6$), is an amphiphilic molecule with a sulfate headgroup.[33] SDS forms micelles in solution with a CMC of ~8 mM; SDS aggregation may impact BSA binding.[34]

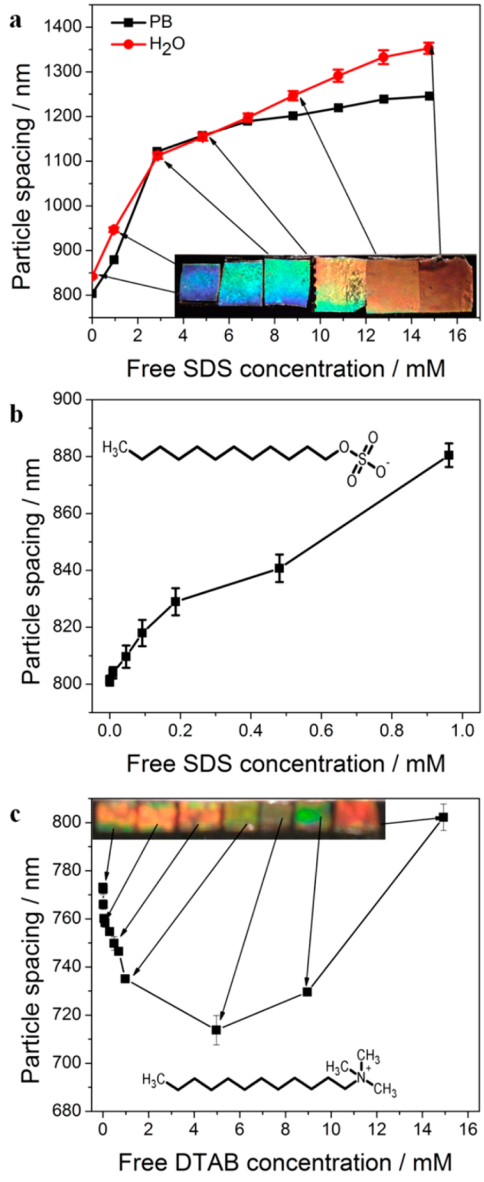

Figure 3. 2D CCA-BSA hydrogel surfactant binding. (a) Free SDS concentration dependence of particle spacing of 2D CCA-BSA hydrogel in pure water at pH 5.83, and in 50 mM PB at pH 8.0. (b) Lower concentration range free SDS concentration dependence and (c) free DTAB concentration dependence of particle spacing of 2D CCA-BSA hydrogel in 50 mM PB (pH 8.0). The insets show photographs of the forward diffraction taken with the camera along the normal and the source below at an angle of 70° to the 2D array normal.

In pure water, the 2D CCA-BSA protein hydrogel in the absence of SDS shows a particle spacing of 820 nm at pH 5.83. The particle spacing increases to 950 nm at 0.96 mM free SDS

dx.doi.org/10.1021/ac404134t | Anal. Chem. 2014, 86, 4840−4847

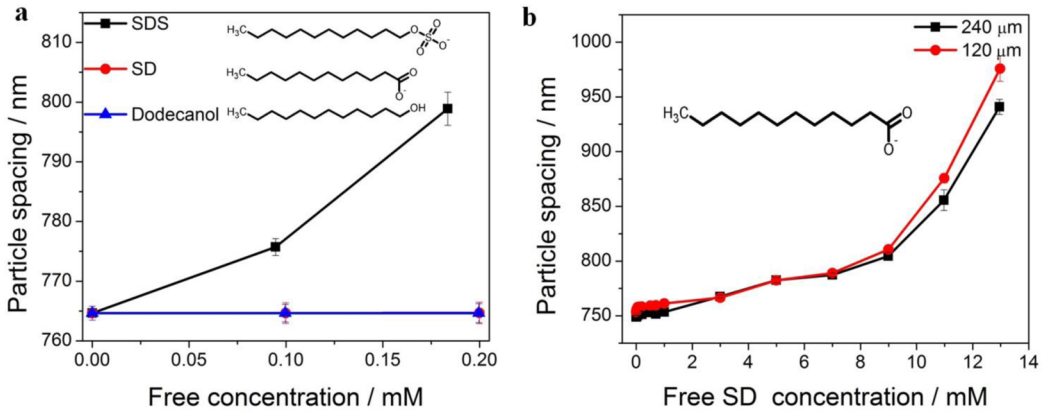

Figure 4. 2D CCA-BSA protein hydrogel fatty acid binding. (a) Free SDS, SD, and dodecanol concentration dependence of the 2D CCA-BSA hydrogel particle spacing in 50 mM PB at pH 8. (b) Free SD concentration dependence of the 2D CCA-BSA hydrogel particle spacing in 50 mM PB at pH 8 (hydrogel thicknesses are 120 and 240 μm).

in solution, while at 14.79 mM SDS, the BSA hydrogel swells, increasing the particle spacing to 1350 nm while the measured unbuffered SDS solution pH is 5.97. The binding of the SDS anions results in a Donnan potential that causes BSA hydrogel swelling.[17,32] Figure 3a also shows the SDS concentration dependence of the particle spacing in 50 mM PB (pH 8.0). The response in 50 mM PB is qualitatively similar to that in pure water indicating only the expected modest response attenuation because of the increased PB ionic strength.

The 2D CCA-BSA hydrogel acts a Coulometer. Thus, we can calculate the number of SDS molecules bound to BSA from the dependence of the BSA hydrogel 2D diffraction on the pH induced change in the net charge. The response sensitivity at pH 8 in 50 mM PB is ~5.5 nm/charge as calculated between pH 6 and 8.5 (Figure 2d and see Supporting Information for the calculation of charge sensitivity). Thus, the 354 nm increase in particle spacing between 0 and 4.83 mM SDS, is estimated to result from binding of ~64 SDS molecules to each BSA at 4.83 mM free SDS. Similarly we calculate that ~14 SDS molecules bind to each BSA at 0.96 mM free SDS. There may exist some saturation in the BSA binding as the SDS concentration exceeds the CMC. We calculate that the detection limit of our BSA hydrogel for SDS binding is 60 μM. It is important to note that our fluorescence measurements of the BSA Trp indicate similar SDS binding for BSA in the hydrogels as for BSA monomer in solution (Supporting Information Figures S6 and S7).[35]

We compared the BSA hydrogel binding of the postively charged surfactant DTAB, whose hydrocarbon chain length is identical to that of SDS, but whose headgroup is positively charged. Figure 3c shows that, in contrast to the monotonic swelling because of anionic SDS binding to the 2D CCA-BSA, binding of positively charged DTAB first shrinks the hydrogel reaching a minimum at 4.97 mM, and then swells with further increases in the DTAB concentration. This is exactly that expected, since at low concentrations at pH = 8 PB, the BSA is negatively charged; the addition of positively charged DTAB decreases the absolute value of net charge toward zero, which shrinks the hydrogel, decreasing the particle spacing (Figure 2). Additional binding of DTAB will then increase the positive net charges, causing the BSA hydrogel to swell.

In addition, the BSA hydrogel binding of a nonionic surfactant that has an identical tail group as SDS and DTAB, was also investigated ($C_{12}E_8$). As expected, it is found that our 2D CCA-BSA photonic crystal protein hydrogel does not change volume upon binding this nonionic surfactant (Supporting Information Figure S8).

2D CCA-BSA Protein Hydrogel SD Fatty Acid Binding. BSA transports hydrophobic molecules in the bloodstream.[36] For example, BSA utilizes greater than six high-affinity fatty binding sites to transport fatty acids to the liver.[33,37] We were initially surprised to find little response of our 2D CCA-BSA hydrogels to SD binding as shown in Figure 4a that compares the responses to SD, dodecanol and SDS under the same experimental conditions. The BSA binding affinity for SD is reported to be 2.3×10^5 for 0.1 wt % BSA at 2 °C.[33] We expect similar binding affinities for SDS, SD and dodecanol since the tail group dominates the affinity; these molecules have identical tail groups. We are confident that both SD and dodecanol bind strongly to BSA since we observe similar quenching of BSA hydrogel Trp fluorescence upon binding of these species to the hydrogel at very low concentrations.

Since SD binding to BSA has a large association constant, we conclude that SD must be binding as a predominantly neutral species similar to dodecanol. It was previously shown that SD at concentrations below the CMC occurs as solution aggregates with dramatically increased carboxyl group pK_a values.[38]

SD binding, however, does increase the particle spacing from 749 to 753 nm between 0 and 1 mM concentrations (Figure 4b) indicating some binding of charged species. Figure 4b also shows that response of our BSA hydrogels is not limited by diffusion equilibration since thinner hydrogels do not respond faster.

2D CCA-BSA/HSA Protein Hydrogel Drug Binding. Serum albumins bind and transport a broad range of drugs in the bloodstream.[36] Our 2D CCA-BSA Coulometer sensor can easily detect the binding of charged drug molecules in solution. For example, Figure 5a shows the detection of the drug picosulfate which is used as a colorectal cleansing agent prior to diagnostic procedures and surgery.[39] Figure 5a shows the picosulfate concentration dependence of the 2D CCA-BSA particle spacing in 50 mM PB (pH 8). At the lowest 8 μM concentrations measured, we estimate that ~0.5 picosulfate molecules are bound per BSA molecule (see Supporting Information for the calculation of number of molecules binding). We estimate that there are ~2 very high affinity binding sites for picosulfate. In addition, the increasing particle spacings at higher picosulfate concentrations indicate additional lower affinity binding sites.

dx.doi.org/10.1021/ac404134t | Anal. Chem. 2014, 86, 4840−4847

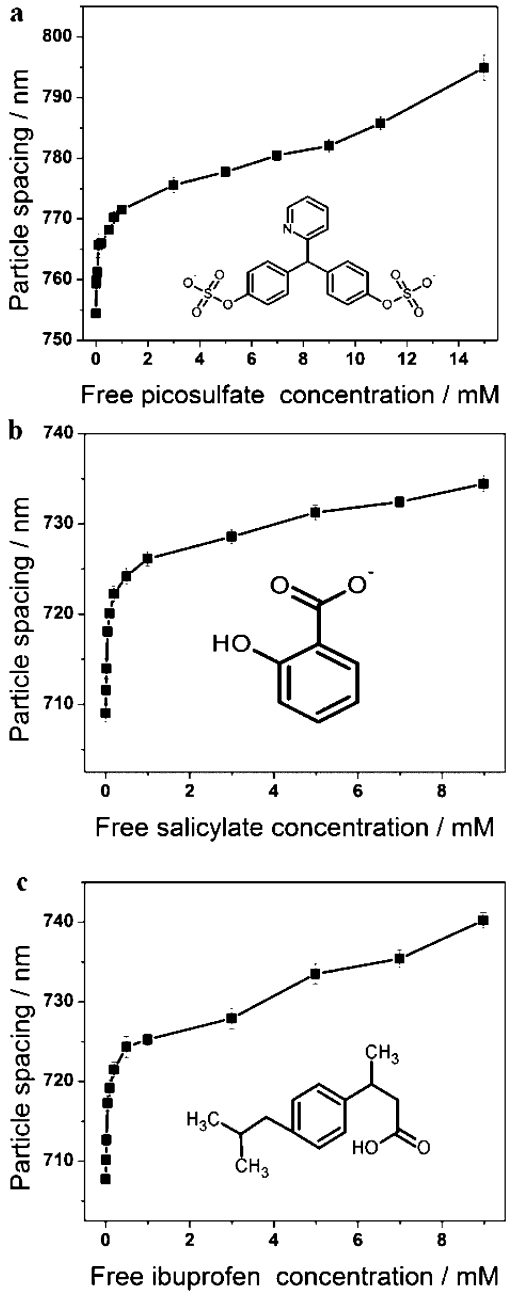

Figure 5. 2D CCA-BSA/HSA protein hydrogel drug binding. (a) Free picosulfate dependence, (b) free salicylate, and (c) free ibuprofen concentration dependence of 2D CCA-HSA hydrogel particle spacings in 50 mM PB (pH 8.0).

The 2D CCA-HSA binds the analgesic and antipyretic drug salicylate, as well as the nonsteroidal anti-inflammatory drug, ibuprofen that is used to treat rheumatoid arthritis and osteoarthroses. Salicylate and ibuprofen are reported to have HSA association constants of 2.2×10^5 and 2.73×10^6 with single HSA high affinity binding sites and several lower affinity binding sites at pH 7.4 at 37 °C.[40,41] These drugs are anionic with salicylic acid pK_a values of 2.97 and ibuprofen pK_a values of 4.91.

These 2D CCA-HSA hydrogels show similar increases in their particle spacings for salicylate and Ibuprofen, with ~3 nm particle spacing increases occurring at the lowest concentrations measured (at ~10 μM free drug). The 3 nm particle spacing increase suggests that ~half of the HSA molecules bind a salicylate or Ibuprofen (Figure 5b, c and see Supporting Information for the calculation of number of molecules binding). We also estimate that HSA has ~3 high affinity binding sites for salicylate and ibuprofen. We roughly calculate binding affinities of $K = 1.2 \times 10^5$ in 50 mM PB at room temperature for both salicylate and ibuprofen. These values differ from those reported for the monomeric HSA protein as measured by Brown and Whitlam.[40,41] However, the previous solution conditions and the temperatures differ from those of our measurements.

2D CCA-BSA Protein Hydrogel Ca^{2+} Binding. Calcium ion (Ca^{2+}) binding to serum albumins has been extensively investigated because of its physiological importance.[42−44] There are at least 30 different BSA Ca^{2+} binding sites with different association constants between 90 and 100 at 37 °C in unbuffered solutions at pH 7.4 and ionic strength ~0.15 M.[44] Figure 6 shows the $CaCl_2$ and NaCl concentration dependence

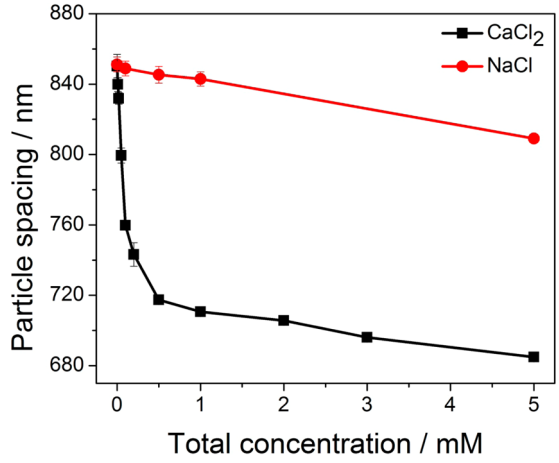

Figure 6. Ca^{2+} and NaCl concentration dependence of the particle spacing of the 2D CCA-BSA protein hydrogel in pure water.

of the 2D CCA-BSA hydrogel particle spacing in pure water. In pure water, the particle spacing decreases from 850 to 685 nm as the Ca^{2+} concentration increases to 5 mM. The Ca^{2+} detection limit is 10 μM. Figure 6 also shows that the particle spacing decreases much less, to 810 nm in the presence of 5 mM NaCl concentrations. This indicates that the increasing ionic strengths have only a minor impact on the particle spacings.

At neutral pH, BSA possesses 11 negative charges. If electrostatics dominated the Ca^{2+} binding response the BSA hydrogel would initially shrink as the net charge goes through zero; further Ca^{2+} binding would increase the net positive charge causing the hydrogel to swell. The sharp Ca^{2+} monotonic shrinkage indicates that the Donnan potential is much less important than polydentate Ca^{2+} binding induced BSA cross-linking within and between the BSA proteins that shrink the hydrogel.

Impact of Hydrogel Cross-Linking on BSA Protein Structure. We expect that the ligand binding affinities of the hydrogel BSA is essentially identical to those in the monomeric proteins because of our gentle cross-linking chemistry. We also directly compared the hydrogel to the monomer solution protein secondary structure and the Trp environment by measuring the 204 nm excited UVRR spectra (Figure 7a) and the 295 nm excited Trp fluorescence emission spectra (Figure

dx.doi.org/10.1021/ac404134t | Anal. Chem. 2014, 86, 4840−4847

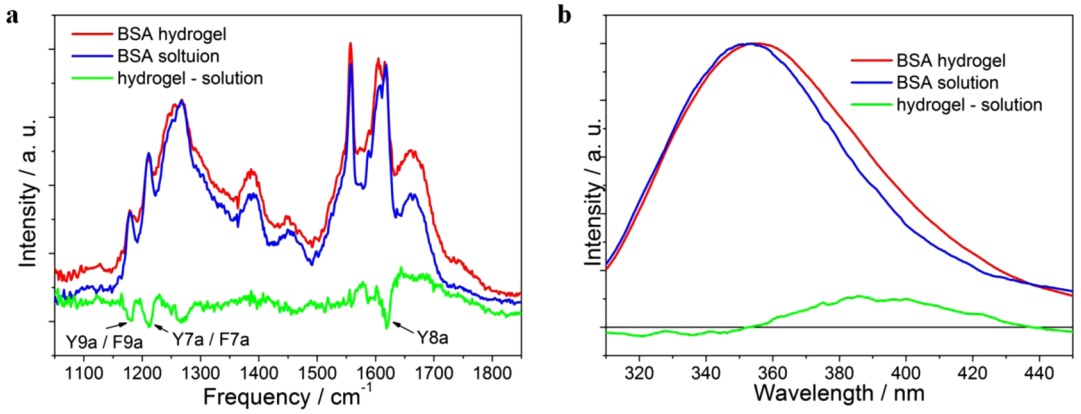

Figure 7. UVRR and fluorescence spectra. (a) 204 nm excited UVRR spectra of BSA hydrogel, monomer solution and UVRR difference between BSA hydrogel and solution. (b) Fluorescence spectra of BSA hydrogel, monomer solution, and difference between BSA hydrogel and solution.

7b). The UVRR spectra are dominated by amide vibrations associated with the peptide backbone, since excitation at 204 nm is resonant with the amide $\pi \rightarrow \pi^*$ transition.[45] The 204 nm excitation is also in resonance with the aromatic side chains (Trp, Tyr, Phe, and His) $B_{a,b}$ transitions and the Arg low-lying $\pi \rightarrow \pi^*$ transition.

The UVRR spectra of the BSA hydrogel and BSA in solution are very similar indicating that their conformations are essentially the same. The ∼1388 and ∼1268 cm^{-1} features derive from the conformationally sensitive the C_α-H and Amide III (AmIII) bands, respectively.

The sharp bands at 1618, 1606, 1588, 1211, and 1179 cm^{-1} are assigned to the Y8a, Y8b/F8a, F8b, Y7a/F7a, and Y9a/F9a vibrations, respectively.[46,47] These aromatic amino acids UVRR bands are sensitive to local environment, and their Raman cross sections have been previously correlated with changes in solvent accessibility.[48,49] The negative features in the difference spectrum show that the Y8a, Y7a/F7a, and Y9a/F9a bands decrease their intensities between the monomer solution and the hydrogel. This indicates that these residues are in a more hydrophilic environment in hydrogel relative to BSA's monomer state in solution. The 1557 cm^{-1} band, has a contribution from O_2 stretching. The broad band at ∼1449 cm^{-1} derives from the overtone of the Arg side chain guanidinium CN_3 out-of-plane bending.[50]

The Trp fluorescence spectrum (Figure 7b) also indicates that the Trp residues in BSA are more exposed to the aqueous environment in the hydrogel compared to the solution monomer state, as evidenced by the bathochromic shift in the Trp emission maximum for the hydrogel.[51] Thus, the UVRR and fluorescence emission spectra indicate that there is a small tertiary structure perturbation of the BSA in the hydrogel. However, the overall structure is preserved; Trp fluorescence changes on surfactant binding are essentially identical for the hydrogel compared to the BSA native monomer.

CONCLUSIONS

We developed a novel photonic crystal protein hydrogel Coulometer whose volume depends sensitively on changes in the protein absolute net charge due to charged analyte binding. The resulting volume changes shift the diffraction of a 2D array attached to the protein hydrogel surface. We demonstrate a diffraction shift of ∼5.5 nm/charge for a 2D photonic crystal BSA protein hydrogel sensor. These protein hydrogels can be fabricated in the future to be even more responsive by decreasing their cross-linking. These protein hydrogels also detect multidentate binding of metals such as Ca^{2+} that form protein hydrogel cross-links.

The work here now enables the use of the broad library of proteins that selectively bind numerous species for sensing. Further, this system can be utilized to screen protein drug targets by measuring the response of the targeted protein hydrogels to different drug molecules to determine the number of binding sites and their affinities.

The 2D diffraction from this photonic crystal hydrogel sensor allows the visual detection of analyte binding and can be used to monitor specific hazardous species present in the environment. The photonic crystal protein hydrogel sensor developed here represents a technology platform for developing future highly selective biosensors. It should be easy to modify the hydrogel cross-linking to increase the responsivity of these hydrogel sensors to specific analytes.

ASSOCIATED CONTENT

Supporting Information

Additional text and data, Figures S1−S8, and Table S1 and additional references. This material is available free of charge via the Internet at http://pubs.acs.org.

AUTHOR INFORMATION

Corresponding Author

*E-mail: asher@pitt.edu.

Notes

The authors declare no competing financial interest.

ACKNOWLEDGMENTS

The authors are grateful for the financial support from HDTRA (Grant 1-10-1-0044). We thank Prof. Marcel Tabak and Dr. Xuegong Lei for helpful discussion.

REFERENCES

(1) Hendrickson, G. R.; Smith, M. H.; South, A. B.; Lyon, L. A. *Adv. Funct. Mater.* **2010**, *20*, 1697−1712.
(2) De, M.; Rana, S.; Akpinar, H.; Miranda, O. R.; Arvizo, R. R.; Bunz, U. H. F.; Rotello, V. M. *Nat. Chem.* **2009**, *1*, 461−465.
(3) Cao, Q.; Rogers, J. A. *Adv. Mater.* **2009**, *21*, 29−53.
(4) Shin, J.; Braun, P. V.; Lee, W. *Sens. Actuators, B* **2010**, *150*, 183−190.
(5) Ge, J.; Yin, Y. *Angew. Chem., Int. Ed.* **2011**, *50*, 1492−1522.
(6) Erickson, D.; Mandal, S.; Yang, A. H. J.; Cordovez, B. *Microfluid. Nanofluid.* **2008**, *4*, 33−52.

(7) Albert, K. J.; Lewis, N. S.; Schauer, C. L.; Sotzing, G. A.; Stitzel, S. E.; Vaid, T. P.; Walt, D. R. *Chem. Rev.* **2000**, *100*, 2595−2626.
(8) Sailor, M. J.; Link, J. R. *Chem. Commun.* **2005**, *0*, 1375.
(9) Woodka, M. D.; Brunschwig, B. S.; Lewis, N. S. *Langmuir* **2007**, *23*, 13232−13241.
(10) Yang, J.-S.; Swager, T. M. *J. Am. Chem. Soc.* **1998**, *120*, 11864−11873.
(11) Weissman, J. M.; Sunkara, H. B.; Tse, A. S.; Asher, S. A. *Science* **1996**, *274*, 959−960.
(12) Holtz, J. H.; Asher, S. A. *Nature* **1997**, *389*, 829−832.
(13) Liu, L.; Li, P.; Asher, S. A. *Nature* **1999**, *397*, 141−144.
(14) Tikhonov, A.; Kornienko, N.; Zhang, J.-T.; Wang, L.; Asher, S. A. *J. Nanophotonics* **2012**, *6*, 063509−1.
(15) Zhang, J.-T.; Wang, L.; Luo, J.; Tikhonov, A.; Kornienko, N.; Asher, S. A. *J. Am. Chem. Soc.* **2011**, *133*, 9152−9155.
(16) Zhang, J.-T.; Wang, L.; Lamont, D. N.; Velankar, S. S.; Asher, S. A. *Angew. Chem., Int. Ed.* **2012**, *51*, 6117−6120.
(17) Zhang, J.-T.; Smith, N.; Asher, S. A. *Anal. Chem.* **2012**, *84*, 6416−6420.
(18) Ehrick, J. D.; Luckett, M. R.; Khatwani, S.; Wei, Y.; Deo, S. K.; Bachas, L. G.; Daunert, S. *Macromol. Biosci.* **2009**, *9*, 864−868.
(19) Hendrickson, G. R.; Andrew Lyon, L. *Soft Matter* **2009**, *5*, 29−35.
(20) Sui, Z.; King, W. J.; Murphy, W. L. *Adv. Funct. Mater.* **2008**, *18*, 1824−1831.
(21) Gu, Z.; Zhao, M.; Sheng, Y.; Bentolila, L. A.; Tang, Y. *Anal. Chem.* **2011**, *83*, 2324−2329.
(22) Ehrick, J. D.; Deo, S. K.; Browning, T. W.; Bachas, L. G.; Madou, M. J.; Daunert, S. *Nat. Mater.* **2005**, *4*, 298−302.
(23) Carter, D. C.; Ho, J. X. In *Advances in Protein Chemistry*; Anfinsen, C. B., Edsall, J. T., Richards, F. M., Eisenberg, D. S., Eds.; Academic Press: San Diego, CA, 1994; Vol. *45*, p 153.
(24) Caillard, R.; Remondetto, G. E.; Mateescu, M. A.; Subirade, M. *J. Food Sci.* **2008**, *73*, C283−C291.
(25) Mi, L.; Fischer, S.; Chung, B.; Sundelacruz, S.; Harden, J. L. *Biomacromolecules* **2005**, *7*, 38−47.
(26) Guan, D.; Ramirez, M.; Shao, L.; Jacobsen, D.; Barrera, I.; Lutkenhaus, J.; Chen, Z. *Biomacromolecules* **2013**, *14*, 2909−2916.
(27) Reese, C. E.; Asher, S. A. *J. Colloid Interface Sci.* **2002**, *248*, 41−46.
(28) Lumsdon, S. O.; Kaler, E. W.; Velev, O. D. *Langmuir* **2004**, *20*, 2108−2116.
(29) Pan, F.; Zhang, J.; Cai, C.; Wang, T. *Langmuir* **2006**, *22*, 7101−7104.
(30) Bykov, S.; Lednev, I.; Ianoul, A.; Mikhonin, A.; Munro, C.; Asher, S. A. *Appl. Spectrosc.* **2005**, *59*, 1541.
(31) Peters Jr., T. In *All About Albumin*; Academic Press: San Diego, CA, 1995; p 9.
(32) Xu, X.; Goponenko, A. V.; Asher, S. A. *J. Am. Chem. Soc.* **2008**, *130*, 3113−3119.
(33) Reynolds, J. A.; Herbert, S.; Steinhardt, J. *Biochemistry* **1968**, *7*, 1357−1361.
(34) Dominguez, A.; Fernandez, A.; Gonzalez, N.; Iglesias, E.; Montenegro, L. *J. Chem. Educ.* **1997**, *74*, 1227.
(35) Gelamo, E. L.; Silva, C. H. T. P.; Imasato, H.; Tabak, M. *Biochim. Biophys. Acta, Protein Struct. Mol. Enzymol.* **2002**, *1594*, 84−99.
(36) Kragh-Hansen, U. *Pharmacol. Rev.* **1981**, *33*, 17−53.
(37) Spector, A. A. *J. Lipid Res.* **1975**, *16*, 165−179.
(38) Kanicky, J. R.; Poniatowski, A. F.; Mehta, N. R.; Shah, D. O. *Langmuir* **1999**, *16*, 172−177.
(39) Hoy, S.; Scott, L.; Wagstaff, A. *Drugs* **2009**, *69*, 123−136.
(40) Brown, K. F.; Crooks, M. J. *Biochem. Pharmacol.* **1976**, *25*, 1175−1178.
(41) Whitlam, J. B.; Crooks, M. J.; Brown, K. F.; Veng Pedrrsen, P. *Biochem. Pharmacol.* **1979**, *28*, 675−678.
(42) Saroff, H. A.; Lewis, M. S. *J. Phys. Chem.* **1963**, *67*, 1211−1216.
(43) Fogh-Andersen, N. *Clin. Chem.* **1977**, *23*, 2122−2126.
(44) Pedersen, K. O. *Scand. J. Clin. Lab. Inv.* **1971**, *28*, 459−469.
(45) Oladepo, S. A.; Xiong, K.; Hong, Z.; Asher, S. A.; Handen, J.; Lednev, I. K. *Chem. Rev.* **2012**, *112*, 2604.
(46) Asher, S. A.; Ludwig, M.; Johnson, C. R. *J. Am. Chem. Soc.* **1986**, *108*, 3186.
(47) Ludwig, M.; Asher, S. A. *J. Am. Chem. Soc.* **1988**, *110*, 1005.
(48) Chi, Z.; Asher, S. A. *J. Phys. Chem. B* **1998**, *102*, 9595.
(49) Xu, M.; Ermolenkov, V. V.; Uversky, V. N.; Lednev, I. K. *J. Biophotonics* **2008**, *1*, 215.
(50) Hong, Z.; Wert, J.; Asher, S. A. *J. Phys. Chem. B* **2013**, *117*, 7145.
(51) Gorinstein, S.; Goshev, I.; Moncheva, S.; Zemser, M.; Weisz, M.; Caspi, A.; Libman, I.; Lerner, H.; Trakhtenberg, S.; Martín-Belloso, O. *J. Protein Chem.* **2000**, *19*, 637.